

Slope-Assisted Brillouin Optical Correlation-Domain Reflectometry Using Polymer Optical Fibers With High Propagation Loss

Heeyoung Lee, Neisei Hayashi, Yosuke Mizuno, *Member, IEEE*, and Kentaro Nakamura, *Member, IEEE*

Abstract—We have recently developed slope-assisted Brillouin optical correlation-domain reflectometry (SA-BOCDR) for higher speed distributed measurement of strain and temperature. However, no reports have been published yet on the use of high-loss fibers. Here, we implement SA-BOCDR using a high-loss polymer optical fiber (POF) for the first time. Due to the gradual reduction in the transmitted power along the POF, the measurement sensitivities are found to depend on sensing position. This unique effect is investigated experimentally, and then a correct POF-based distributed measurement is performed by compensating this effect.

Index Terms—Brillouin scattering, distributed measurement, optical fiber sensors, polymer optical fibers.

I. INTRODUCTION

FIBER-OPTIC distributed sensing based on Brillouin scattering [1] has been regarded as one of the most important techniques to detect damages of civil infrastructures. A variety of its configurations developed so far can be classified into five categories: Brillouin optical time-domain reflectometry (BOTDR) [2]–[5], Brillouin optical correlation-domain reflectometry (BOCDR) [6]–[15], Brillouin optical time-domain analysis (BOTDA) [16]–[21], Brillouin optical frequency-domain analysis (BOFDA) [22]–[24], and Brillouin optical correlation-domain analysis (BOCDA) [25]–[29]. Each configuration, with its own advantages and disadvantages, has been extensively studied to enhance the performance. Here, among them, we focus on BOCDR, which is the only technique that can simultaneously achieve intrinsically single-end accessibility and high spatial resolution.

Since the first proposal of BOCDR [6], a number of schemes have been implemented to improve its performance, such as the measurement range [7], [8], spatial resolution [9], [10], and

sampling rate [11]. One of the newly developed configurations is slope-assisted (SA-) BOCDR [12], which uses the power of the Brillouin gain spectrum (BGS) to derive the Brillouin frequency shift (BFS), leading to a high sampling rate, loss-point detectability, and beyond-nominal resolution effect [13]. Its fundamental operation has been well investigated when low-loss silica glass fibers are used as fibers under test (FUTs) [12], but no reports have been provided on how the performance is affected by use of high-loss FUTs, including tellurite glass fibers [9], chalcogenide fibers [30], and polymer optical fibers (POFs) [14], [15]. At the sacrifice of the shortened measurement range, the use of such high-loss fibers provides BOCDR with some advantages, such as stronger Brillouin signals (for tellurite [9] and chalcogenide fibers [30]) (leading to enhanced spatial resolution), extended upper limit of detectable strain [14] and much higher temperature sensitivity [15] (for POFs). Thus, it is of crucial importance to investigate the influence of the use of high-loss fibers on SA-BOCDR operation.

In this work, employing POFs as high-loss fibers, we demonstrate high-speed distributed sensing based on SA-BOCDR. We show that, in contrast to the case of low-loss silica fibers, the strain and temperature sensitivities are dependent on sensing position because the transmitted power is gradually reduced in the POFs. After analyzing this unique effect experimentally, we show that this effect can be compensated so that a correct POF-based distributed measurement using SA-BOCDR can be performed.

II. PRINCIPLES

When light propagates in an optical fiber, due to the interaction with acoustic phonons, backscattered Stokes light is generated through Brillouin scattering. The central frequency of the Stokes light spectrum (i.e., BGS) is lowered than that of the incident light spectrum. This central frequency downshift is referred to as BFS, which is about ~ 10.8 GHz for silica single-mode fibers (SMFs) [1] and ~ 2.8 GHz for perfluorinated POFs [14] when the incident light wavelength is 1550 nm. When strain or temperature change is applied to the fiber, the BFS shifts to higher or lower frequency depending on the fiber types. Their strain- and temperature-dependence coefficients are reported to be approximately 500 MHz/% and 1 MHz/K for silica SMFs [31], [32] and -120 MHz/% and -3 MHz/K for POFs [15], [32]. These dependences have been widely exploited as a basic

Manuscript received November 25, 2016; revised January 23, 2017; accepted January 26, 2017. Date of publication February 1, 2017; date of current version April 20, 2017. This work was supported in part by the JSPS KAKENHI Grants 25709032, 26630180, and 25007652, and in part by research grants from the Japan Gas Association, the ESPEC Foundation for Global Environment Research and Technology, and the Association for Disaster Prevention Research.

H. Lee, Y. Mizuno, and K. Nakamura are with the Institute of Innovative Research, Tokyo Institute of Technology, Yokohama 226-8503, Japan (e-mail: hylee@sonic.pi.titech.ac.jp; ymizuno@sonic.pi.titech.ac.jp; knakamur@sonic.pi.titech.ac.jp).

N. Hayashi is with the Research Center for Advanced Science and Technology, The University of Tokyo, Tokyo 153-8503, Japan (e-mail: hayashi@cntp.t.u-tokyo.ac.jp).

Color versions of one or more of the figures in this paper are available online at <http://ieeexplore.ieee.org>.

Digital Object Identifier 10.1109/JLT.2017.2663440

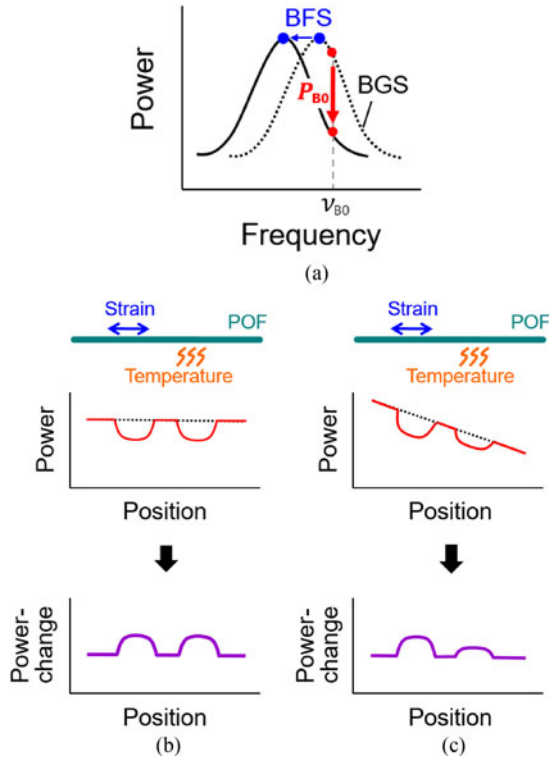


Fig. 1. (a) Schematic of the operating principle of SA-BOCDR. (b) and (c) Power and power-change distributions along (b) a low-loss fiber and (c) a high-loss fiber; with (solid curves) and without (dotted lines) partial strain and heat.

sensing mechanism of fiber-optic distributed Brillouin sensors, including BOCDR.

BOCDR enables distributed measurement using a so-called correlation peak inside the FUT [6], [10], [33]. The correlation peak can be generated by sinusoidally modulating the output frequency of the laser; the position of the correlation peak can be scanned along the FUT by sweeping the modulation frequency f_m . In general, due to the nature of sinusoidal frequency modulation, multiple correlation peaks are periodically generated along the FUT, which limits the measurement range d_m as [10]

$$d_m = \frac{c}{2nf_m}, \quad (1)$$

where c is the velocity of light in vacuum and n is the core refractive index. The spatial resolution Δz is given by [10]

$$\Delta z = \frac{c \Delta \nu_B}{2\pi n f_m \Delta f}, \quad (2)$$

where $\Delta \nu_B$ is the Brillouin bandwidth and Δf is the modulation amplitude. Note that Eq. (2) holds true only when f_m is lower than $\Delta \nu_B$ [10].

Standard BOCDR acquires the whole BGS to derive the BFS at a single sensing position (as a peak frequency of the BGS) [6], [10] which is relatively time-consuming. In contrast, SA-BOCDR operates based on the spectral power change at a fixed frequency ν_{B0} by exploiting its one-to-one correspondence to the BFS (see Fig. 1(a)) [12], which enables high-speed measurement. Note that the BFS of the FUT needs to be mea-

sured beforehand in SA-BOCDR to optimize the measurement sensitivity and/or dynamic range. One unique feature of SA-BOCDR is that its final output (i.e., a power-change distribution along the FUT) does not directly reproduce the actual BFS distribution, while the output of standard BOCDR completely reproduces it. As described in detail in [13], the power-change distribution in SA-BOCDR basically shows a trapezoidal shape, and only when the length of strained or heated section is equal to the theoretical spatial resolution, it shows a triangular shape. In addition, SA-BOCDR has a unique ability to detect strained or heated sections even shorter than the nominal resolution calculated by Eq. (2) [13].

When a silica SMF with a low propagation loss is used as an FUT, unless the FUT is extremely long, the Brillouin power shows almost no change irrespective of the sensing position (see Fig. 1(b)). However, when a relatively high-loss fiber is used, even when the FUT is short, the Brillouin power decreases with increasing distance from the proximal end of the FUT (i.e., the pigtail end of the second port of a circulator) as shown in Fig. 1(c). Note that the final system output of SA-BOCDR is provided as a power-change distribution, and strain (or heat) is displayed as a positive shift in the vertical axis. The weakening of the BGS along the high-loss fiber leads to the reduction in the spectral slope, finally resulting in the gradual decrease in the strain and temperature sensitivities.

III. EXPERIMENTAL SETUP

We employed a 15.0-m-long perfluorinated graded-index POF as an FUT. The POF had a three-layered structure consisting of core, cladding, and overcladding (diameters: 50, 70, and 490 μm , respectively). A propagation loss of the POF was ~ 250 dB/km at 1550 nm.

The experimental setup of POF-based SA-BOCDR (refer to Fig. 3 in [12]) is basically the same as that of standard BOCDR [6] except for the electrical signal processing. All the light paths except the FUT are composed of silica SMFs. As a light source, a laser diode at 1550 nm with a bandwidth of ~ 1 MHz was used. Its output was divided into two light beams: pump and reference. The pump light was amplified to ~ 25 dBm using an erbium-doped fiber amplifier (EDFA) and injected into the FUT. The backscattered Stokes light was amplified to ~ 1 dBm using another EDFA. The reference light was guided through a ~ 1 -km-long delay fiber, amplified to ~ 2 dBm, and then coupled with the Stokes light for heterodyne detection. Using a polarization controller, the polarization state was adjusted so that the signal-to-noise ratio (SNR) became maximal for each measurement (note that the use of a polarization scrambler for observing Brillouin signals in POFs causes considerable reduction in SNR [34]). The optical beat signals were converted into electrical signals using a photo diode and observed using an electrical spectrum analyzer (ESA).

Subsequently, exploiting the narrow band-pass filtering function of the ESA (video bandwidth: 10 kHz; resolution bandwidth: 10 MHz), the change in the spectral power at ν_{B0} was sequentially output to an oscilloscope (OSC). As a preparatory experiment for determining the ν_{B0} value and the bandwidth of

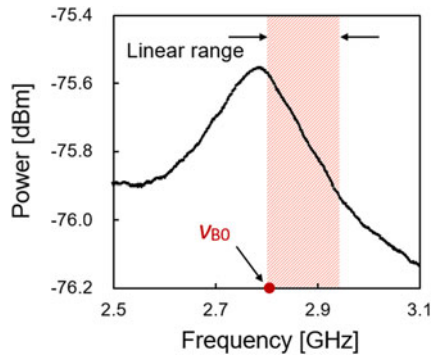


Fig. 2. Local BGS obtained at 1.0 m away from the proximal POF end.

the linear region, we measured the local BGS obtained at 1.0 m away from the proximal POF end (see Fig. 2). The detailed measurement conditions are described in the next paragraph. The BFS was 2.76 GHz at room temperature (25 °C). The optimal v_{B0} value was found to be 2.80 GHz, which was set to a higher frequency than the BFS because the BGS shifts to lower frequency in POFs with strain and/or heating [15] (unlike the case of silica-SMF-based SA-BOCDR). The bandwidth of the linear region (refer to [12] for its definition) was approximately 140 MHz (2.80–2.94 GHz), which corresponds to the strain of up to $\sim 1.15\%$ and the temperature change of ~ 43 °C in the POF (with light propagation, the BGS is basically weakened in the vertical direction; in other words, if normalized, the BGS shows an only negligible change depending on the location, leading to almost no position dependence of the linear range). Here we discuss the shape of the BGS, which is neither Lorentzian nor symmetrical. Compared to silica fibers, POFs inherently have a much wider Brillouin bandwidth (>100 MHz) [14]. Moreover, in general, as the modulation amplitude grows higher, the Brillouin bandwidth becomes wider [10], which deviates the BGS from a Lorentzian shape. Meanwhile, the asymmetric shape originates from the overlap of the foot of the Rayleigh spectrum [34], which also grows wider by modulation in the same manner as the BGS [10]. Note that the BFS of the POF (~ 2.8 GHz) is ~ 4 times lower than that of silica fibers [14] and that the BGS is more likely to be overlapped by the Rayleigh spectrum.

In the preceding measurement as well as in the following experiments, the modulation frequency f_m and amplitude Δf were set to 6.15–6.33 MHz and 0.6 GHz, respectively, corresponding to the measurement range of 18.1 m and the theoretical spatial resolution of 0.96 m according to (1) and (2). The repetition rate was set to 100 Hz, and averaging was performed 128 times on the OSC to improve the SNR.

IV. EXPERIMENTAL RESULTS

First, to derive the theoretical strain and temperature sensitivities as functions of sensing position, we measured the BGS distribution along the POF with a constant interval of 1.0 m using standard BOCDR (see Fig. 3). Due to the high propagation loss in the POF, the peak power of the BGS gradually decreased with light propagation, which also induced the reduction in its spectral slope. Note that the BGS is weakened even within the

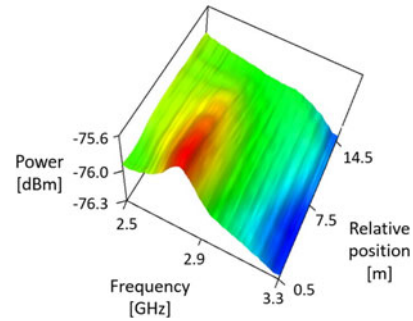


Fig. 3. BGS distribution along the POF.

fiber length of the spatial resolution, resulting an unavoidable measurement error. Here we interpreted the measured sensitivity as that of the midpoint of the corresponding fiber section.

By differentiating the spectral slope in the linear range ($v_{B0} = 2.80$ – 2.94 GHz), the theoretical dependence of the sensitivity on sensing position was derived (see Fig. 4(a)). The slope decreased almost linearly as the sensing position became far from the proximal POF end with a coefficient of approximately -0.16 dB/GHz/m, which corresponds to the strain sensitivity dependence of -1.99×10^{-2} dB/%/m and the temperature sensitivity dependence of -5.22×10^{-4} dB/°C/m. Subsequently, we measured the spectral power dependence on sensing position when the temperature of the POF was locally changed to 60 °C. The spectral powers were measured when 1.0-m-long sections (4 sections; 2.0–3.0, 5.0–6.0, 8.0–9.0, 11.0–12.0 m distant from the proximal POF end) were heated, and plotted as functions of temperature (see Fig. 4(b)). The measured data were in good agreement with the theoretical trends (indicated by dotted lines) obtained from the BGS distributions (see Fig. 3). The spectral powers were almost linearly dependent on temperature, and their coefficients were found to decrease with increasing distance from the proximal POF end. For each section, the temperature sensitivity was calculated and plotted as a function of sensing position (see Fig. 4(c)). The dependence coefficient was -4.98×10^{-4} dB/°C/m (corresponding to -2.10×10^{-2} dB/%/m for strain), which is in good agreement with the theoretical value calculated from the BGS distribution (-5.22×10^{-4} dB/°C/m).

Finally, we demonstrated distributed measurement of strain and temperature along the POF using SA-BOCDR. The structure of the FUT is depicted in Fig. 5(a). A 1.0-m-long section (close to the nominal spatial resolution) was strained for 1%, and another 1.0-m-long section was heated to 60 °C. The measured power-change distribution is shown in Fig. 5(b). At the expected sections, the power changes corresponding to the strain and the temperature change were observed, which moderately agrees with the theoretical dotted line considering the sensitivity dependence on sensing position and the trapezoidal effect of SA-BOCDR [13]. Thus, the applied strain and temperature change were correctly detected. The measurement errors originate from the signal fluctuations caused by the low SNR, which can be improved by increasing the number of averaging, increasing the pump power, or optimizing the low-pass filtering function of the ESA.

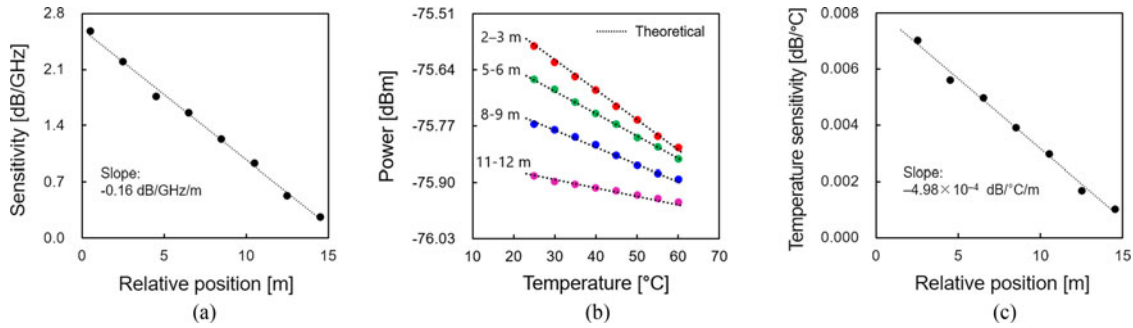


Fig. 4. (a) Sensitivity plotted as a function of sensing position for theoretical analysis. The dotted line is a linear fit. (b) Spectral powers plotted as functions of temperature; measured at four different sections in the POF. The dotted lines are theoretical trends. (c) Temperature sensitivity plotted as a function of sensing position. The dotted line is a linear fit.

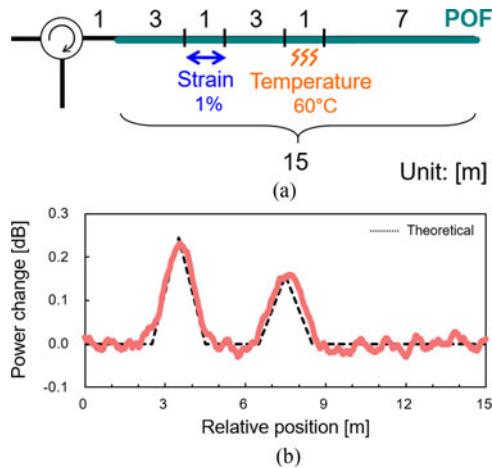


Fig. 5. (a) Structure of the fiber under test for final demonstration. (b) Power-change distributions along the sensing fiber. The dotted line is a theoretical trend.

V. CONCLUSION

We investigated the performance of SA-BOCDR using a POF with a relatively high propagation loss (~ 250 dB/km at 1550 nm). The measurement sensitivity was shown to be dependent on the sensing position in the POF. The dependence coefficients were -2.10×10^{-2} dB/%/m for strain and -4.98×10^{-4} dB/°C/m for temperature, which agreed well with the theoretical predictions. By compensating this influence, we successfully demonstrated a distributed strain and temperature measurement along the POF with a spatial resolution of ~ 1 m. We believe that these results will be an important archive in implementing SA-BOCDR using high-loss fibers, especially POFs, for high-speed distributed strain and temperature sensing with high flexibility and high temperature sensitivity.

REFERENCES

- [1] G. P. Agrawal, *Nonlinear Fiber Optics*. San Diego, CA, USA: Academic, 1995.
- [2] T. Kurashima, T. Horiguchi, H. Izumita, S. Furukawa, and Y. Koyamada, "Brillouin optical-fiber time domain reflectometry," *IEICE Trans. Commun.*, vol. E76-B, no. 4, pp. 382–390, Apr. 1993.
- [3] Q. Li, J. Gan, Y. Wu, Z. Zhang, J. Li, and Z. Yang, "High spatial resolution BOTDR based on differential Brillouin spectrum technique," *IEEE Photon. Technol. Lett.*, vol. 28, no. 14, pp. 1493–1496, Jul. 2016.
- [4] F. Wang, W. Zhan, X. Zhang, and Y. Lu, "Improvement of spatial resolution for BOTDR by iterative subdivision method," *J. Lightw. Technol.*, vol. 31, no. 23, pp. 3663–3667, Dec. 2013.
- [5] D. Iida and F. Ito, "Detection sensitivity of Brillouin scattering near Fresnel reflection in BOTDR measurement," *J. Lightw. Technol.*, vol. 26, no. 4, pp. 417–424, Feb. 2008.
- [6] Y. Mizuno, W. Zou, Z. He, and K. Hotate, "Proposal of Brillouin optical correlation-domain reflectometry (BOCDR)," *Opt. Exp.*, vol. 16, no. 16, pp. 12148–12153, Aug. 2008.
- [7] Y. Mizuno, Z. He, and K. Hotate, "Measurement range enlargement in Brillouin optical correlation-domain reflectometry based on temporal gating scheme," *Opt. Exp.*, vol. 17, no. 11, pp. 9040–9046, May 2009.
- [8] Y. Mizuno, Z. He, and K. Hotate, "Measurement range enlargement in Brillouin optical correlation-domain reflectometry based on double-modulation scheme," *Opt. Exp.*, vol. 18, no. 6, pp. 5926–5933, Mar. 2010.
- [9] Y. Mizuno, Z. He, and K. Hotate, "Distributed strain measurement using a tellurite glass fiber with Brillouin optical correlation-domain reflectometry," *Opt. Commun.*, vol. 283, no. 11, pp. 2438–2441, Feb. 2010.
- [10] Y. Mizuno, W. Zou, Z. He, and K. Hotate, "Operation of Brillouin optical correlation-domain reflectometry: Theoretical analysis and experimental validation," *J. Lightw. Technol.*, vol. 28, no. 22, pp. 3300–3306, Nov. 2010.
- [11] Y. Mizuno, N. Hayashi, H. Fukuda, K. Y. Song, and K. Nakamura, "Ultrahigh-speed distributed Brillouin reflectometry," *Light, Sci. Appl.*, vol. 5, Dec. 2016, Art. ID e16184.
- [12] H. Lee, N. Hayashi, Y. Mizuno, and K. Nakamura, "Slope-assisted Brillouin optical correlation-domain reflectometry: Proof of concept," *IEEE Photon. J.*, vol. 8, no. 3, Jun. 2016, Art. ID 6802807.
- [13] H. Lee, N. Hayashi, Y. Mizuno, and K. Nakamura, "Operation of slope-assisted Brillouin optical correlation-domain reflectometry: Comparison of system output with actual frequency shift distribution," *Opt. Exp.*, vol. 24, no. 25, pp. 29190–29197, Dec. 2016.
- [14] Y. Mizuno and K. Nakamura, "Experimental study of Brillouin scattering in perfluorinated polymer optical fiber at telecommunication wavelength," *Appl. Phys. Lett.*, vol. 97, no. 2, Jul. 2010, Art. ID 021103.
- [15] Y. Mizuno and K. Nakamura, "Potential of Brillouin scattering in polymer optical fiber for strain-insensitive high-accuracy temperature sensing," *Opt. Lett.*, vol. 35, no. 23, pp. 3985–3987, Dec. 2010.
- [16] T. Horiguchi and M. Tateda, "BOTDA-nondestructive measurement of single-mode optical fiber attenuation characteristics using Brillouin interaction: Theory," *J. Lightw. Technol.*, vol. 7, no. 8, pp. 1170–1176, Aug. 1989.
- [17] Y. Peled, A. Motil, L. Yaron, and M. Tur, "Slope-assisted fast distributed sensing in optical fibers with arbitrary Brillouin profile," *Opt. Exp.*, vol. 19, no. 21, pp. 19845–19854, Oct. 2011.
- [18] Y. Dong *et al.*, "High-spatial-resolution fast BOTDA for dynamic strain measurement based on differential double-pulse and second-order sideband of modulation," *IEEE Photon. J.*, vol. 5, no. 3, Jun. 2013, Art. ID 2600407.
- [19] M. A. Soto, S. L. Floch, and L. Thévenaz, "Bipolar optical pulse coding for performance enhancement in BOTDA sensors," *Opt. Lett.*, vol. 21, no. 14, pp. 16390–16397, Jul. 2013.

- [20] R. Bernini, A. Minardo, and L. Zeni, "Dynamic strain measurement in optical fibers by stimulated Brillouin scattering," *Opt. Lett.*, vol. 34, no. 17, pp. 2613–2615, Sep. 2009.
- [21] Y. Dong, P. Xu, H. Zhang, Z. Lu, L. Chen, and X. Bao, "Characterization of evolution of mode coupling in a graded-index polymer optical fiber by using Brillouin optical time-domain analysis," *Opt. Exp.*, vol. 22, no. 22, pp. 26510–26516, Nov. 2014.
- [22] D. Garus, K. Krebber, and F. Schliep, "Distributed sensing technique based on Brillouin optical-fiber frequency-domain analysis," *Opt. Lett.*, vol. 21, no. 17, pp. 1402–1404, Sep. 1996.
- [23] A. Wosniok, Y. Mizuno, K. Krebber, and K. Nakamura, "L-BOFDA: A new sensor technique for distributed Brillouin sensing," in *Proc. 5th Eur. Workshop Opt. Fibre Sens.*, Krakow, Poland, 2013, vol. 8794, pp. 8794–8798.
- [24] R. Bernini, A. Minardo, and L. Zeni, "Distributed sensing at centimeter-scale spatial resolution by BOFDA: Measurements and signal processing," *IEEE Photon. J.*, vol. 4, no. 1, pp. 48–56, Feb. 2012.
- [25] K. Hotate and T. Hasegawa, "Measurement of Brillouin gain spectrum distribution along an optical fiber using a correlation-based technique—Proposal, experiment and simulation," *IEICE Trans. Electron.*, vol. E83-C, no. 3, pp. 405–412, Mar. 2000.
- [26] Y. H. Kim, K. Lee, and K. Y. Song, "Brillouin optical correlation domain analysis with more than 1 million effective sensing points based on differential measurement," *Opt. Exp.*, vol. 23, no. 26, pp. 33241–33248, Dec. 2015.
- [27] W. Zou, C. Jin, and J. Chen, "Distributed strain sensing based on combination of Brillouin gain and loss effects in Brillouin optical correlation domain analysis," *Appl. Phys. Exp.*, vol. 5, no. 8, Jul. 2012, Art. ID 082503.
- [28] R. Cohen, Y. London, Y. Antman, and A. Zadok, "Brillouin optical correlation domain analysis with 4 millimeter resolution based on amplified spontaneous emission," *Opt. Exp.*, vol. 22, no. 10, pp. 12070–12078, May 2014.
- [29] J. H. Jeong, K. Lee, K. Y. Song, J. M. Jeong, and S. B. Lee, "Differential measurement scheme for Brillouin optical correlation domain analysis," *Opt. Exp.*, vol. 20, no. 24, pp. 27094–27101, Nov. 2012.
- [30] K. S. Abedin, "Observation of strong stimulated Brillouin scattering in single-mode As₂Se₃ chalcogenide fiber," *Opt. Exp.*, vol. 13, no. 25, pp. 10266–10271, Dec. 2005.
- [31] T. Horiguchi, T. Kurashima, and M. Tateda, "Tensile strain dependence of Brillouin frequency shift in silica optical fibers," *IEEE Photon. Technol. Lett.*, vol. 1, no. 5, pp. 107–108, May 1989.
- [32] T. Kurashima, M. Tateda, and M. Tateda, "Thermal effects on the Brillouin frequency shift in jacketed optical silica fibers," *Appl. Opt.*, vol. 29, no. 15, pp. 2219–2222, May 1990.
- [33] K. Hotate and Z. He, "Synthesis of optical-coherence function and its applications in distributed and multiplexed optical sensing," *J. Lightw. Technol.*, vol. 24, no. 7, pp. 2541–2557, Jul. 2006.
- [34] Y. Mizuno, N. Hayashi, and K. Nakamura, "Polarisation state optimisation in observing Brillouin scattering signal in polymer optical fibres," *IEICE Electron. Lett.*, vol. 49, no. 1, pp. 56–57, Jan. 2013.

Heeyoung Lee was born in Seoul, South Korea, on August 21, 1990. She received the B.E. degree in mechanical engineering from Kyungpook National University, Daegu, South Korea, in 2014. Since 2015, she has been working toward the M.E. degree in fiber-optic sensors at Tokyo Institute of Technology, Tokyo, Japan.

Her research interests include fiber-optic sensing and polymer optics. Ms. Lee is a Member of the Japanese Society of Applied Physics.

Neisei Hayashi was born in Gunma, Japan, on April 13, 1988. He received the B.E. degree in advanced production from Gunma National College of Technology, Maebashi, Japan, in 2011, and the M.E. and Dr. Eng degrees in information processing from Tokyo Institute of Technology, Tokyo, Japan, in 2013 and 2015, respectively.

From 2013 to 2015, he was involved in polymer fiber sensing for his Dr. Eng. degree with Tokyo Institute of Technology. Also from 2013 to 2015, he was a Research Fellow (DC1) of the Japan Society for the Promotion of Science (JSPS). Since 2016, he has been continuing to study fiber sensing as a Research Fellow (PD) of JSPS with The University of Tokyo, Tokyo, Japan. His research interests include fiber-optic sensing, polymer optics, and nonlinear optics.

Mr. Hayashi received the TELECOM System Technology Award for Student in 2012, the Seiichi Tejima Doctoral Dissertation Award in 2015, and the NF Foundation R&D Encouragement Award in 2016. He is a Member of the Japanese Society of Applied Physics and the Institute of Electronics, Information, and Communication Engineers of Japan.

Yosuke Mizuno (M'14) was born in Hyogo, Japan, on October 13, 1982. He received the B.E., M.E., and Dr. Eng. degrees in electronic engineering from The University of Tokyo, Tokyo, Japan, in 2005, 2007, and 2010, respectively.

From 2007 to 2010, he was involved in Brillouin optical correlation-domain reflectometry for his Dr. Eng. degree with The University of Tokyo. From 2007 to 2010, he was a Research Fellow (DC1) of the Japan Society for the Promotion of Science. From 2010 to 2012, as a Research Fellow (PD) of JSPS, he worked on polymer optics with Tokyo Institute of Technology, Tokyo, Japan. In 2011, he stayed with BAM Federal Institute for Materials Research and Testing, Germany, as a Visiting Research Associate. Since 2012, he has been an Assistant Professor with the Precision and Intelligence Laboratory (currently, Institute of Innovative Research), Tokyo Institute of Technology, where he is active in fiber-optic sensing, polymer optics, and ultrasonics.

Dr. Mizuno received the Funai Research Award in 2010, the Ando Incentive Prize for the Study of Electronics in 2011, the NF Foundation R&D Encouragement Award in 2012, the Tokyo Tech Challenging Research Award in 2013, the Konica Minolta Imaging Science Award in 2014, the Japanese Society of Applied Physics (JSAP) Young Scientist Presentation Award in 2015, and the ESPEC Prize for the Encouragement of Environmental Studies in 2016. He is a Member of the IEEE Photonics Society, the JSAP, and the Institute of Electronics, Information, and Communication Engineers of Japan.

Kentaro Nakamura (M'00) was born in Tokyo, Japan, on July 3, 1963. He received the B.E., M.E., and Dr. Eng. degrees from Tokyo Institute of Technology, Tokyo, Japan, in 1987, 1989, and 1992, respectively.

Since 2010, he has been a Professor with the Precision and Intelligence Laboratory (currently, Institute of Innovative Research), Tokyo Institute of Technology. His research interests include applications of ultrasonic waves, measurement of vibration and sound using optical methods, and fiber-optic sensing.

Prof. Nakamura received the Awaya Kiyoshi Award for encouragement of research from the Acoustical Society of Japan (ASJ) in 1996, and the Best Paper Awards from the Institute of Electronics, Information and Communication Engineers (IEICE) in 1998 and from the Symposium on Ultrasonic Electronics in 2007 and 2011, respectively. He also received the Japanese Journal of Applied Physics Editorial Contribution Award from the Japan Society of Applied Physics (JSAP) in 2007. He is a Member of the IEEE, the ASJ, the JSAP, the IEICE, and the Institute of Electrical Engineers of Japan.